RMIT UNIVERSITY

Thank you for downloading this document from the RMIT Research Repository.

The RMIT Research Repository is an open access database showcasing the research outputs of RMIT University researchers.

RMIT Research Repository: http://researchbank.rmit.edu.au/

PLEASE DO NOT REMOVE THIS PAGE

Bistatic DIAL for Multi-Species Aviation Pollutant Measurements from RPAS

Alessandro Gardi, Roberto Sabatini
RMIT University – SAMME, Melbourne, Australia

Abstract

This paper presents the conceptual design of a new low-cost measurement system for the determination of pollutant concentrations associated with aircraft operations. The proposed system employs Light Detection and Ranging (LIDAR) and passive electro-optics equipment installed in two non-collocated components. The source component consists of a tuneable small-size and low-cost/weight LIDAR emitter, which can be installed either on airborne or ground-based autonomous vehicles, or in fixed surface installations. The sensor component includes a target surface calibrated for reflectance and passive electro-optics equipment calibrated for radiance, both installed on an adjustable support. The proposed bistatic system determines the column-averaged molecular and aerosol pollutant concentrations along the LIDAR beam by measuring the cumulative absorption and scattering phenomena along the optical slant range. The molecular column densities are measured by means of Differential Absorption LIDAR (DIAL), which exploits the known molecular vibration processes for non-ambiguous species detection. Aerosol concentrations such as particulate and soot are determined by means of knowledge-based inversion with regularization. The laboratory calibration of the system components is also discussed. Previously published uncertainty analysis results highlighted the positive qualities of the proposed measurement system even in degraded meteorological conditions, making the proposed bistatic LIDAR a viable alternative to other systems currently employed.

Introduction

The steady growth of air transport worldwide is posing new challenges to policy-makers, scientists and operators as the already unsustainable environmental impacts are predicted to further increase not only in their absolute values but also in their share of the overall man-made emissions. In particular, the Intergovernmental Panel on Climate Change (IPCC) originally estimated the aviation-related carbon dioxide (CO_2) emissions to be between 2% and 3% of global anthropogenic CO_2 emissions [1]. Due to the sustained growth rates, this figure is already being revised [2] and is expected to increase by 50% over current levels by 2050 [3]. Policy-makers and researchers around the world are thus increasingly committed to revert the unsustainable trends. Major aerospace and aviation modernisation programmes launched in the recent years, including Clean Sky, NextGen, SESAR, Greener by Design, Environmentally Responsible Aviation, are therefore focusing on a number of strategies to reduce environmental impacts of transport aircraft in the future. Hydrocarbon-based fuels are particularly addressed since they represent by far the largest energy source for aircraft propulsion. The combustion of hydrocarbon fuels produces a number of noxious compounds as well as greenhouse gases, of which CO_2 is the principal representative, being the largest component of exhaust emissions. As a reference, assuming an average chemical composition of $C_{12}H_{23}$ [4], each kilogram of typical Jet-A1 fuel can develop up to 3.16 kilograms of CO_2, therefore the total carbon-related radiative forcing impact of each single commercial flight is considerable. The legislation currently in place for noise pollution control and charging is expected to be gradually extended to CO_2 and possibly other pollutants in the future, possibly exploiting suitable forms of Emission Trading Schemes (ETS). The real-time and continuous monitoring of emissions will significantly enhance the effectiveness, equity and overall viability of ETS for aviation [5], therefore, it is envisioned that large airports and high air traffic density areas will likely be monitored in terms of pollutant emissions.

Current research activities are addressing new sensor technologies and measurement techniques for the determination of aviation pollutant concentrations. The new systems should feature either: greater operational flexibility, better sensitivity, accuracy, precision, reliability, greater spectral/spatial/temporal resolutions, and reduced weight/volume/costs. The research community is interested, in particular, in the spatial and temporal variations of macroscopic observables, and on the microphysical and chemical properties of atmospheric constituents and pollutants, including molecular, aerosol and particulate species [6, 7]. An accurate measurement of CO_2 concentration variations in space and time related to aircraft operations is particularly important. Recently developed powerful LIDAR systems with low weight and packaged in relatively small casings, are ideally suited for the development of measurement systems targeting the column densities of various important molecular species, including carbon oxides (CO_X), nitrogen oxides (NO_X), sulphur dioxides (SO_X), O_2 and ozone (O_3), both locally and over extended geographic areas [8, 9].

Measurement System Concept

The conceptual design of the bistatic measurement system was initially proposed in [10], based on previous research [11-14]. As depicted in Fig. 1, the proposed system consists of a LIDAR emitter installed on a Remotely Piloted Aircraft System (RPAS) or on fixed/movable surface installations, and a sensor component.
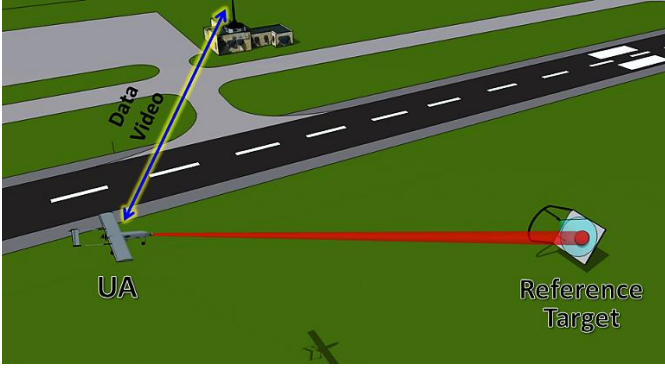
Figure 1. Representation of the bistatic LIDAR system, not to scale.

The sensor component consists of a target surface featuring high and diffused reflectance and exhibiting Lambertian behaviour, such as Spectralon™, and a visible/infrared camera mounted on a rail. The RPAS platform flies pre-determined trajectories based on the required space and time frames of the measurement. Fig. 2 depicts the payload bay of a recent variant of the AEROSONDE RPAS, which will serve as the initial reference for the system components design.

Figure 2. Payload bay of a recent variant of the AEROSONDE RPAS.

In [10] we introduced the key features of the measuring system and discussed the rationale supporting its development. A calibration technique was also introduced, employing a second ground-based LIDAR emitter and electro-optics photo-detectors. This article reviews and updates our research results, discussing a laboratory calibration of the system components.

Atmospheric Propagation

The propagation of laser radiation in atmosphere is affected by a number of linear and nonlinear effects. Assuming a Gaussian profile of the laser beam at the source and an average focused irradiance, the following expression identifies the dependencies of the peak irradiance I_P, on absorption, scattering, diffraction, jitter, atmospheric turbulence and thermal blooming effects [13, 15]:

$$I_P(z,\lambda) = \frac{b(z)\,\tau(z,\lambda)\,P(\lambda)}{\pi\left(a_d^2(z,\lambda) + a_j^2(z) + a_t^2(z,\lambda)\right)} \tag{1}$$

where z is the linear coordinate along the beam, λ is the wavelength, $P(\lambda)$ is the transmitted laser power, b is the blooming factor, $\tau(z,\lambda)$ is the transmittance coefficient, which accounts for absorption and scattering associated with all molecular and aerosol species present in the path. The 1/e beam radiuses associated with diffraction, $a_d(z,\lambda)$, beam jitter, $a_j(z)$, and turbulence, $a_t(z,\lambda)$, can be calculated as [7, 15]:

$$a_d(z,\lambda) = \frac{Q z \lambda}{2\pi a_0} \tag{2}$$

$$a_j^2(z) = 2\langle\Theta_x^2\rangle z^2 \tag{3}$$

$$a_t(z,\lambda) = \frac{2\,C_N^{6/5} z^{8/5}}{\lambda^{1/5}} \tag{4}$$

where Q is the beam quality factor, a_o is the beam $1/e$ radius, $\langle\Theta_x^2\rangle$ is the variance of the single axis jitter angle that is assumed to be equal to $\langle\Theta_y^2\rangle$, and C_N^2 is the refractive index structure constant. An empirical model for the blooming factor $b(z)$, which is the ratio of the bloomed I_B to unbloomed I_{UB} peak irradiance, is:

$$b(z) = \frac{I_B}{I_{UB}} = \frac{1}{1 + 0.0625\,N^2(z)} \tag{5}$$

N is the thermal distortion parameter, calculated as:

$$N(z) = \frac{-n_T\,\alpha_m\,P\,z^2}{\pi\,d_0\,v_0\,c_P\,a_0^3} \cdot \left[\frac{2}{z^2}\int_0^R \frac{a_0}{a(z')}dz' \int_0^{z'} \frac{a_0^2\,v_0\,\tau''}{a}\,dz''\right] \tag{6}$$

where v_o is the uniform wind velocity in the weak attenuation limit ($\gamma z \ll 1$), n_T, d_o, and c_p are, respectively, the coefficients of index change with respect to temperature, density, and specific heat at constant pressure. The transmittance coefficient τ depends on the integral effect of absorption and scattering phenomena, both for molecular and aerosol species, on the entire beam length.

Retrieval of Molecular Species

When referring to the integral absorption and scattering due to specific molecular species, it is possible to adopt the following expression of the transmittance:

$$\tau(z,\lambda) = e^{-\int_0^z \gamma(z,\lambda)\,dz} = e^{-\int_0^z \sum_i [\psi_i(\lambda)\,\cdot n_i(z)]\,dz} \tag{7}$$

where:

$\psi_i(\lambda)$ = cross-section of the ith species

n_i = molecular volume density of the ith species

The retrieval of molecular species is based on the Differential Absorption LIDAR (DIAL) technique. In particular, the laser source emits beams at two predefined wavelengths, of which the first (λ_{ON}) is selected in correspondence of a major vibrational band of the targeted pollutant molecule (*on-absorption line*), clear from the transition/vibration spectrum of other atmospheric components. The second wavelength (λ_{OFF}) is selected outside the vibrational band (*off-absorption line*) so that the difference in cross-sections, $\Delta\psi \triangleq \psi(\lambda_{ON}) - \psi(\lambda_{OFF})$ in association with the targeted pollutant is maximised. A number of databases and atmospheric Radiative Transfer Model (RTM) codes are available and allow an accurate estimation of the propagation spectrum for identifying the optimal combination of DIAL wavelengths based on the mentioned criteria. The RTM codes adopted in this research are freely available and based on the HITRAN database (acronym for High Resolution Transmission), as documented in [12]. The functional block diagram of the bistatic DIAL measurement system is represented in Fig. 3.
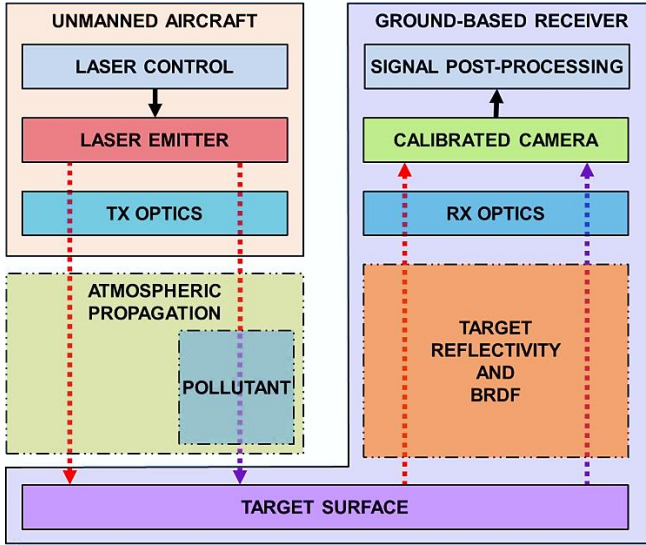
Figure 3. Functional block diagram of the bistatic measurement system performing the retrieval of molecular pollutant species by means of the DIAL technique.

From Eq. 7, the fraction between the measured incident laser energy associated with the on-absorption line of pollutant species P and the one associated with the off-absorption line, $R_{ON/OFF}$, can be expressed as [10]:

$$R_{ON/OFF} = \frac{E(\lambda_{ON})}{E(\lambda_{OFF})} = \frac{\tau_{ON}}{\tau_{OFF}} = e^{-[\psi_P(\lambda_{ON})-\psi_P(\lambda_{OFF})]\int_0^D n_P(r)\,dr} \qquad (8)$$

where D is the total beam length. The total pollutant column density N_P, which is the integral of the molecular volume density on the entire beam, is therefore:

$$N_P = \int_0^D n_P(r)\,dr = \frac{-\ln(R_{ON/OFF})}{\Delta\psi} \qquad (9)$$

The average molecular volume concentration of the pollutant on the path, $\tilde{n}_P$, is therefore:

$$\tilde{n}_P = \frac{N_P}{D} = \frac{-\ln(R_{ON/OFF})}{D \cdot \Delta\psi} \qquad (10)$$

As evident from Eq. 8 to 10, the DIAL measurement neglects most of the parasite phenomena, as they are assumed to equally affect the off-absorption and the on-absorption transmittances. For the specific carbon dioxide (CO_2) measurement system implementation, a successfully adopted on-absorption wavelength is $\lambda_{ON} = 1572.335\ nm$ [16-22], in the Near-InfraRed (NIR).

Particle Retrieval

The retrieval of aerosol concentrations was originally examined in [12]. As per eq. 1, both molecular and aerosol concentrations in the transmission medium (i.e. the atmosphere) introduce absorption and scattering phenomena that affect the laser beam propagation. Therefore, the atmospheric transmittance measurement data accumulated in a certain time period using passive imaging systems enable the concurrent retrieval of aerosol concentrations. The difficulty in developing inversion algorithms lies in the fact that the input optical data are related to the investigated microphysical parameters through nonlinear integral equations of the first kind (Fredholm equations), which cannot be solved analytically. The

generalised form of the Fredholm equation for atmospheric data retrieval is:

$$\alpha(\lambda), \beta(\lambda) = \int K_{\alpha,\beta}(r, n, k, \lambda) \cdot D(r)dr \qquad (11)$$

where $\alpha(\lambda)$, and $\beta(\lambda)$ represent the optical data, $K_{\alpha,\beta}$ is the atmospheric kernel function (containing information on particle size, refractive index etc.) and $D(r)$ is the particle size distribution. The numerical solution of these equations leads to the so called ill-posed inverse problem. Such problems are characterised by a strong sensitivity of the solution space toward uncertainties of the input data, the non-uniqueness of the solution space, and the incompleteness of the solution space. In fact, the solution space may still be correct in a mathematical sense, but might not necessarily reflect the physical conditions. As the problem cannot be entirely defined by the measurements, a priori knowledge of the state vector is required in order to determine the most probable solution, with a probabilistic Bayesian approach. Let y be the measurement vector containing the measured radiances, and x be the concentration of a given constituent, then the general remote sensing equation can be written as follows [9]:

$$y = f(x, b) + \epsilon \qquad (12)$$

where f represents the forward transfer function, b the other parameters affecting the measurement, and ϵ the measurement noise. In the case of instruments measuring laser radiance, the vector b includes the target surface reflectance and radiance features (BRDF, reflectivity, emissivity and temperature), the variables describing the atmospheric state (vertical turbulence profile, temperature, water vapour and other atmospheric constituents, clouds, aerosols, etc.), and some characteristics of the measurement instruments (spectral response functions and resolution). The inverse problem consists in retrieving $\hat{x}$, an estimate of the true state x, from the measurement y, and can be expressed as:

$$\hat{x} = R(y, \hat{b}) = R(f(x, b) + \epsilon, \hat{b}) \qquad (13)$$

where $\hat{b}$ is an estimate of the non-retrieved parameters b, and R is the inverse transfer function. This a priori information consists of an a priori state vector x_a and its covariance matrix S_a, which may be provided by model simulations. Therefore, the inverse problem can be rewritten as follows:

$$\hat{x} = R(y, \hat{b}, x_a) \qquad (14)$$

Various inversion techniques were proposed. One of the most popular approaches is the inversion with regularisation, offering the advantage of reducing oscillations in the solution that are frequently experienced in data retrieved from electro-optical measurements [6, 15]. This approach consists in introducing constraints, such as derivative analysis (smoothness) of the particle size distribution functions, positive sign of the functions and maximum variations over time. The comprehensive inversion algorithm with regularisation is depicted in Fig. 4.
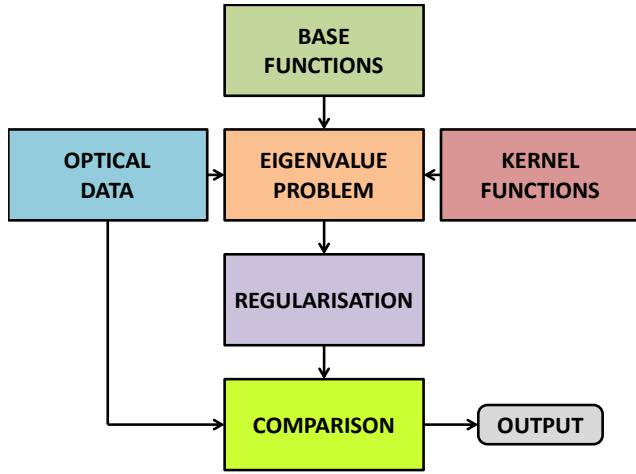
Figure 4. Block diagram of the particle retrieval algorithm [12].

Using appropriate kernel/base functions, this algorithm can deliver parameters such as effective (average) particle radius, particle size distribution, total surface-area concentration, total number/volume concentrations, real and imaginary parts of the refractive index, single scattering albedo, etc. The base functions are Gaussian fits of the existing particle concentration data and are used to reconstruct the investigated particle size distributions. The kernel functions describe the interaction of laser radiation with the atmosphere and contain information about the atmospheric transmittance, including scattering and absorption processes.

Laboratory Calibration

The photo-camera calibration is an experimental procedure that allows determination of the Integrated Radiance Response Function (AIRF) [7, 23]. A highly selective filter (i.e., response centred on the laser wavelength) is used in conjunction with the photo-camera to detect the laser spot energy on the target and to generate a Pixel Intensity Matrix (PIM) in a high resolution greyscale format. The calibration setup is shown in Fig. 5.
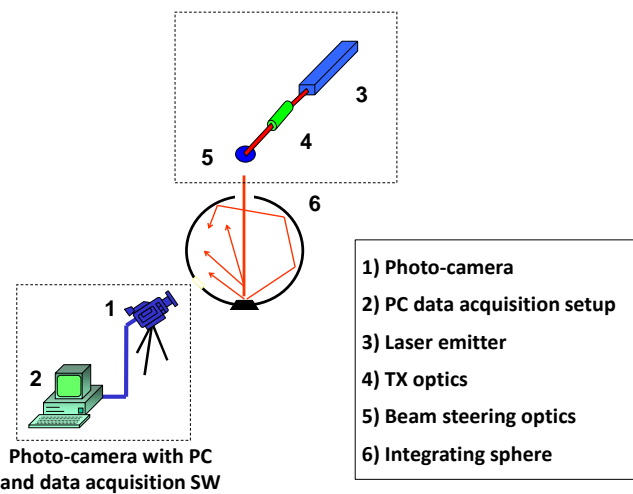

Figure 5. Layout of the photo-camera calibration.

The response of a single pixel in terms of Analogue Digital Unit (ADU) is:

$$ADU_{i,j} \; \propto \; \frac{A}{4 \cdot f_\#^2 + 1} \cdot g \cdot i_{time} \cdot \int_{\lambda_1}^{\lambda_2} (\tau_O \cdot \eta_D \cdot E_S) \, d\lambda \qquad (15)$$

where:

$\lambda_{1,2}$ = limits of the photo-camera spectral band filter
η_D = detector quantum efficiency
E_S = spectral radiance
τ_O = optics transmittance
A = pixel area
g = read-out electronics gain
$f_\#$ = optics f-number
i_{time} = photo-camera integration time

Therefore, the experimental parameters to be controlled during the calibration procedure are the integration time, the optics f-number and other settings of the photo-camera (e.g., the gain of the read-out electronics which may be selected by the operator). Fixing these parameters for a certain interval of integral radiance, it is possible to determine the AIRF of the camera by using an extended reference source. The function (calibration curve) so obtained is then used to determine the values of integral radiance for reconstructing the radiant intensity map of the target. Some mathematical models were developed and experimentally validated to calculate the optimal frame rate of the photo-camera [7]. In particular, photo-cameras are characterised by acquisition frequencies that typically are significantly different from the laser operating PRF. In the bistatic DIAL case, some additional consideration must be given to the alternated wavelengths of different pulses. A conceptual representation of the camera acquisition windows and dark zones in presence of laser pulses of alternating wavelength (different shades of red) is presented in Fig. 6. The parameters describing the train of pulses are the pulse duration (τ), the pulse period (T_P) and the PRF (f). Similarly, the camera image acquisition process is defined by the frame period (T_F) and the camera acquisition time (T_A). Generally T_A is inferior to T_F. The difference between T_F and T_A is the so called camera 'dark-time' (T_{dark}).
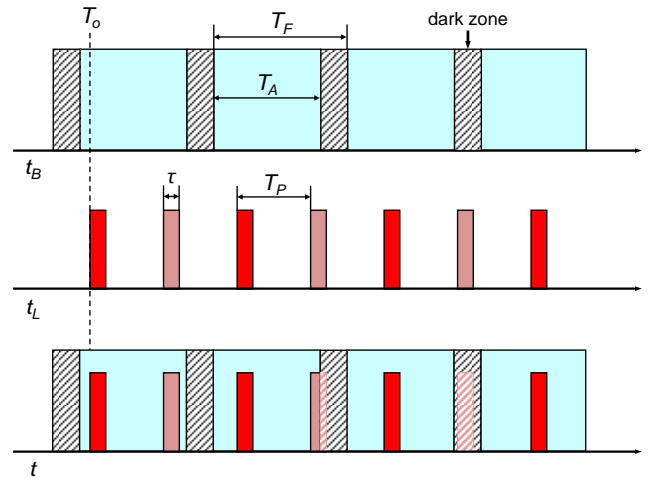

Figure 6. Photo-camera acquisition sequence and laser pulses.

Good synchronisation is extremely difficult even at low PRF and almost impossible as the PRF increases. Therefore a careful analysis is required in order to determine the optimal frame rate for the camera acquisition as a function of known laser pulse parameters. Since the camera frames are not synchronised with the laser pulses, considering the camera acquisition windows sequence as time base (t_B), the instant of arrival of the first laser pulse (reflected from the target) at the camera (T_o) can be treated as a random variable. Example results of a frame rate optimisation analysis, referred to laser emitters operating at $f = 10$ Hz and $f = 40$ kHz are summarised in Fig. 7, where P_{err} is the error probability.
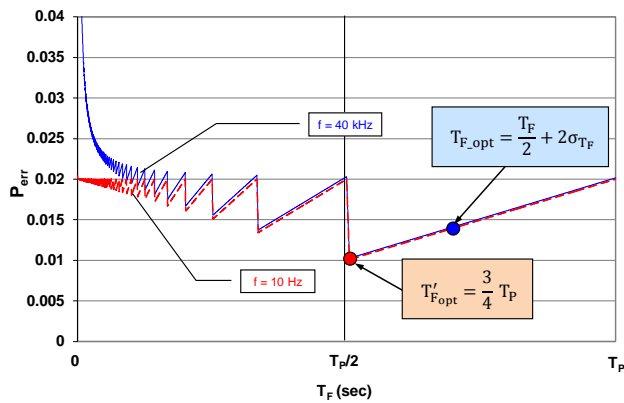
Figure 7.   Results of NIR camera frame rate optimisation analysis

Conclusions

This paper presented the conceptual development of an innovative measurement system for the determination of pollutant concentrations associated with aircraft operations. The system employs Light Detection and Ranging (LIDAR) and passive electro-optics equipment to perform an accurate estimation of column-averaged molecular and aerosol concentrations along the slant optical path, by measuring the cumulative effect of absorption and scattering optical processes along the LIDAR beam. In particular, the molecular column densities are derived by means of the Differential Absorption LIDAR (DIAL) method, exploiting the molecular vibration processes for non-ambiguous species detection. The estimation of aerosol concentrations such as particulate and soot can be obtained, on the other hand, by knowledge-based inversion with regularisation. Carbon dioxide (CO_2) is the primarily addressed molecular pollutant, as its contributions to radiative forcing are a concern for the environmental sustainability of the aviation industry. The bistatic measurement system is specifically conceived to supply fundamental real-time inputs related to the pollution levels to novel Air Traffic Management (ATM) systems, currently researched, for the dynamic reconfiguration of air traffic flows and airspace sectors [24]. A preliminary uncertainty analysis addressing the CO_2 column density measurements confirmed the positive qualities of the proposed system even in degraded meteorological conditions, making it a viable alternative to the relatively more complex and costly monostatic LIDAR systems currently available. Ongoing research activities are extending the system concept of operations to other families of aviation pollutants such as nitrogen oxides (NO_X), sulphur oxides (SO_X), and Volatile Organic Compounds (VOC). This activity will benefit, in particular, from the continuing evolution of small-size and low-weight tuneable laser emitter technology. Further system development phases will involve laboratory testing as well as flight testing in various representative conditions. In particular, the concurrent development and experimental testing activities of other RPAS-based LIDAR systems for Sense-and-Avoid (SAA) applications will be highly synergic [25]. The experimental flight testing activity will be performed in a suitably developed laser test range in full compliance with eye-safety requirements [14, 23].

References

1. Penner J E and al, *Aviation and the Global Atmosphere: A Special Report of IPCC Working Groups I and III in Collaboration with the Scientific Assessment Panel to the Montreal Protocol on Substances that Deplete the Ozone Layer*, Cambridge University Press, 1999.
2. Lee D S, Pitari G, Grewe V, Gierens K, Penner J E, Petzold A*, et al.*, "Transport impacts on atmosphere and climate: Aviation", *Atmospheric Environment,* vol. 44, pp. 4678-4734, 2010. DOI: 10.1016/j.atmosenv.2009.06.005
3. Janić M, *The sustainability of air transportation: a quantitative analysis and assessment*, Ashgate Publishing, Ltd., 2007.
4. Nojoumi H, Dincer I, and Naterer G F, "Greenhouse gas emissions assessment of hydrogen and kerosene-fueled aircraft propulsion", *International Journal of Hydrogen Energy,* vol. 34, pp. 1363-1369, 2009. DOI: 10.1016/j.ijhydene.2008.11.017
5. Wit R C N, Boon B H, van Velzen A, Cames M, Deuber O, and Lee D S, "Giving wings to emission trading - Inclusion of aviation under the European emission trading system (ETS): design and impacts", CE Solutions for environment, economy and technology, Directorate General for Environment of the European Commission ENV.C.2/ETU/2004/0074r, Delft, NL, 2005.
6. Rodgers C D, *Inverse methods for atmospheric sounding: Theory and practice* vol. 2, World scientific Singapore, 2000.
7. Sabatini R and Richardson M A, *Airborne Laser Systems Testing and Analysis*, RTO AGARDograph AG-300 Vol. 26, Flight Test Instrumentation Series, Systems Concepts and Integration Panel (SCI-126), NATO Science and Technology Organization, 2010.
8. Veselovskii I, Kolgotin A, Griaznov V, Müller D, Franke K, and Whiteman D N, "Inversion of multiwavelength Raman lidar data for retrieval of bimodal aerosol size distribution", *Applied Optics,* vol. 43, pp. 1180-1195, 2004. DOI: 10.1029/2003JD003538
9. Müller D, Wagner F, Wandinger U, Ansmann A, Wendisch M, Althausen D*, et al.*, "Microphysical particle parameters from extinction and backscatter lidar data by inversion with regularization: Experiment", *Applied Optics,* vol. 39, pp. 1879-1892, 2000
10. Gardi A, Sabatini R, and Wild G, "Unmanned aircraft bistatic lidar for CO2 colum density determination", in proceedings of *IEEE Metrology for Aerospace (MetroAeroSpace 2014)*, Benevento, Italy, 2014. DOI: 10.1109/MetroAeroSpace.2014.6865892
11. Sabatini R and Richardson M A, "Innovative methods for planetary atmospheric sounding by lasers", in proceedings of *AIAA Space 2008 Conference*, San Diego, CA, USA, 2008. DOI: 10.2514/6.2008-7670
12. Sabatini R, Richardson M A, Jia H, and Zammit-Mangion D, "Airborne laser systems for atmospheric sounding in the near infrared", in proceedings of *SPIE 8433, Laser Sources and Applications, Photonics Europe 2012*, Brussels, Belgium, 2012. DOI: 10.1117/12.915718
13. Sabatini R and Richardson M A, "Novel atmospheric extinction measurement techniques for aerospace laser system applications", *Infrared Physics and Technology,* vol. 56, pp. 30-50, 2013. DOI: 10.1016/j.infrared.2012.10.002
14. Sabatini R, "Innovative Flight Test Instrumentation and Techniques for Airborne Laser Systems Performance Analysis and Mission Effectiveness Evaluation", in proceedings of *IEEE Metrology for Aerospace (MetroAeroSpace 2014)*, Benevento, Italy, 2014, pp. 1-17. DOI: 10.1109/MetroAeroSpace.2014.6865886
15. Gebhardt F G, "High Power Laser Propagation", *Applied Optics,* vol. 15, pp. 1479-1493, 1976
16. Krainak M A, Andrews A E, Allan G R, Burris J F, Riris H, Sun X*, et al.*, "Measurements of atmospheric CO2 over a horizontal path using a tunable-diode-laser and erbium-fiber-amplifier at 1572 nm", in proceedings of *Conference on Lasers and Electro-Optics 2003 (CLEO '03)*, Baltimore, MD, USA, 2003, pp. 878 - 881
17. Riris H, Abshire J B, Allan G, Burris J F, Chen J, Kawa S R*, et al.*, "A laser sounder for measuring atmospheric trace gases from space", in proceedings of *SPIE 6750, Lidar Technologies,*

Techniques, and Measurements for Atmospheric Remote Sensing III, Florence, Italy, 2007. DOI: 10.1117/12.737607

18. Allan G R, Riris H, Abshire J B, Sun X, Wilson E, Burris J F*, et al.*, "Laser sounder for active remote sensing measurements of CO2 concentrations", in proceedings of *IEEE/AIAA Aerospace Conference 2008 (AC2008)*, Big Sky, MT, USA, 2008, pp. 1-7. DOI: 10.1109/AERO.2008.4526387

19. Amediek A, Fix A, Ehret G, Caron J, and Durand Y, "Airborne lidar reflectance measurements at 1.57 μm in support of the A-SCOPE mission for atmospheric CO2", *Atmospheric Measurement Techniques Discussions,* vol. 2, pp. 1487-1536, 2009

20. Abshire J B, Riris H, Allan G R, Weaver C J, Mao J, Sun X*, et al.*, "Pulsed airborne lidar measurements of atmospheric CO2 column absorption", *Tellus, Series B: Chemical and Physical Meteorology,* vol. 62, pp. 770-783, 2010. DOI: 10.1111/j.1600-0889.2010.00502.x

21. Abshire J B, Ramanathan A, Riris H, Mao J, Allan G R, Hasselbrack W E*, et al.*, "Airborne measurements of CO2 column concentration and range using a pulsed direct-detection IPDA lidar", *Remote Sensing,* vol. 6, pp. 443-469, 2013. DOI: 10.3390/rs6010443

22. Abshire J B, Riris H, Weaver C J, Mao J, Allan G R, Hasselbrack W E*, et al.*, "Airborne measurements of CO2 column absorption and range using a pulsed direct-detection integrated path differential absorption lidar", *Applied Optics,* vol. 52, pp. 4446-4461, 2013. DOI: 10.1364/AO.52.004446

23. Sabatini R and Richardson M A, "A new approach to eye-safety analysis for airborne laser systems flight test and training operations", *Optics and Laser Technology,* vol. 35, pp. 191-198, 2003. DOI: 10.1016/S0030-3992(02)00171-8

24. Gardi A, Sabatini R, Kistan T, Lim Y, and Ramasamy S, "4-Dimensional Trajectory Functionalities for Air Traffic Management Systems", in proceedings of *Integrated Communication, Navigation and Surveillance Conference (ICNS 2015)*, Herndon, VA, USA, 2015

25. Sabatini R, Gardi A, Ramasamy S, and Richardson M A, "A Laser Obstacle Warning and Avoidance system for Manned and Unmanned Aircraft", in proceedings of *2014 IEEE International Workshop on Metrology for Aerospace (MetroAeroSpace 2014)*, Benevento, Italy, 2014, pp. 616-621. DOI: 10.1109/MetroAeroSpace.2014.6865998